BMC Nephrology

RESEARCH

Open Access

Measuring bone metabolic activity in dialysis patients with renal osteodystrophy using [^{18}F]-Sodium Fluoride positron emission tomography- comparison between static and dynamic measurements

Louise Aaltonen[1*], Niina Koivuviita[1], Marko Seppänen[2,3], Vesa Oikonen[2], Anna K. Kirjavainen[4], Heikki Kröger[5], Eliisa Löyttyniemi[6] and Kaj Metsärinne[1]

Abstract

Background Dynamic [^{18}F]NaF PET has shown promising results in the measurement of bone metabolism in patients with renal osteodystrophy. Dynamic PET scans are challenging in clinical practice, and the objective of this study was to evaluate whether standardized uptake values measured by [^{18}F]NaF PET could be a feasible method.

Methods Twenty-eight patients on maintenance dialysis with confirmed renal osteodystrophy underwent a dynamic [^{18}F]NaF PET scan. As a reference for bone metabolism, a bone biopsy was obtained from the anterior iliac crest (AIC). Tracer activity in bone was measured using Patlak analysis and standardized uptake values (SUV). SUV was also adjusted to tracer activity measured from the aorta 48–60 min after injection (SUVR).

Results SUV measured in the lumbar spine (L1-L4) and at the AIC did not correlate with histomorphometric parameters obtained by bone biopsy. There was no statistically significant difference between SUV in different turnover groups. When adjusting the mean bone uptake of fluoride in the lumbar spine, there was a strong correlation with the blood clearance of tracer to bone (K_i). SUVR also correlated significantly with histomorphometric markers obtained by bone biopsy.

Conclusions These results suggest that measurements of tracer activity in the blood 48–60 min after tracer injection could be used to correct SUVs from static [^{18}F]NaF PET scans. However, further research and validation of the method is needed.

Keywords [^{18}F]NaF PET, [^{18}F]-sodium fluoride positron emission tomography, Dynamic, Static, Bone histomorphometry, Renal osteodystrophy

*Correspondence:
Louise Aaltonen
louise.aaltonen@tyks.fi

Full list of author information is available at the end of the article

Introduction

Dynamic [^{18}F]-sodium fluoride ([^{18}F]NaF) PET scans are not presently suitable for clinical practice. However, the measurement of standardized bone uptake would be an easier way of implementing the method. [^{18}F]NaF is a sensitive bone-seeking tracer and enables, in an unique way, the measurement of bone turnover [1, 2]. [^{18}F]NaF has a half-life of 110 min and has high and rapid bone uptake and blood clearance [3]. [^{18}F]NaF reflects bone remodeling and osteoblast and osteoclast activity [4–7].

Renal osteodystrophy is present in the majority of patients undergoing maintenance dialysis, and bone abnormalities cause increased morbidity and mortality [8–11]. The treatment of renal osteodystrophy depends on the underlying bone disease. Bone biopsy is the gold standard in the diagnostics of renal osteodystrophy, but invasive, not widely available and is restricted to a single site in the bone [12, 13]. Furthermore, biomarkers diagnostic accuracy is not sufficient in patients with advanced chronic kidney disease (CKD) [8, 14]. [^{18}F]NaF PET has shown promising results in patients with renal osteodystrophy. [^{18}F]NaF correlates with histomorphometric markers of bone turnover and can distinguish between low- and high-turnover bone disease in CKD5D patients [4, 6, 7]. A noninvasive diagnostic tool that could rule out low-turnover bone disease or confirm high-turnover bone disease before surgery or the initiation of medical treatment would be highly welcomed in clinical practice.

Since the bone uptake of [^{18}F]NaF is irreversible during the PET scan as with the widely used [^{18}F]FDG, similar quantification methods can be used. Traditionally, the [^{18}F]NaF concentration in arterial plasma is considered the gold standard input function. The concentration of [^{18}F]NaF in the plasma and blood cells is in balance, and results obtained using plasma and blood are highly correlated. The erythrocyte-to-plasma ratio for fluoride is ~0.43 and is stable for at least 2 h [15]. It is however important to report whether blood or plasma sampling is used, because the time activity curve (TAC) of blood is lower than that of the plasma and using blood TAC as the input function instead of plasma will lead to higher uptake rate estimates. Quantitative dynamic [^{18}F]NaF PET studies often use the method described by Hawkins [1], a three-compartment model, where the bone time-activity curve and the arterial input function (AIF) are analyzed to determine the blood clearance of [^{18}F]NaF to bone. As a more easily performed alternative, the Patlak analysis can be used [16]. Nevertheless, the Patlak method still requires a full dynamic PET scan. The fractional uptake rate (FUR) is an approximation of the outcome of the Patlak method, requiring only a single late PET scan, but full input function from the time of administration is still needed [17].

In most clinical studies investigating [^{18}F]NaF PET and metabolic bone diseases, dynamic PET scans of 60 min have been used. The challenge of dynamic PET scans in clinical practice is the duration of the scan and the need for an AIF. AIF can be measured using an arterial bloodline or substituted with venous blood sampling or noninvasively from the PET image [1, 18]. Arterial cannulation is an invasive procedure and is not very practical in the clinical use in the setting of an imaging study.

A simpler method of quantitative PET study is to measure standardized uptake values (SUV). This requires only a late single scan and obviates the need of blood samples. In this method, tracer radioactivity in the bone region of interest (ROI) is normalized for the mean radioactivity concentration in the body. Therefore, regional SUV is affected by changes in tracer uptake in other tissues and excretion into urine. In local bone diseases, such as bone tumors, [^{18}F]NaF metabolic values and changes in bone metabolism measured by SUV correlate with blood clearance in the dynamic PET scan [19]. However, when evaluating extensive metabolic or metastatic bone disease or the effect of anabolic osteoporosis treatment, clearance of the tracer from blood to bone may be a more reliable indicator of site-specific bone formation [20].

There is also vascular uptake of [^{18}F]NaF [21], and an inverse relationship between the activity of arterial mineral deposition and regional bone metabolism has been documented [22]. Patients with chronic kidney disease have an excessive prevalence of vascular calcification. To what extent this affects standardized bone uptake is unclear.

The objective of this study was to evaluate whether SUVs measured by [^{18}F]NaF PET could be a feasible method to distinguish the subgroups of renal osteodystrophy. Additionally, we sought to evaluate whether the calcification score impacts the correlation between standardized bone uptake, blood clearance to bone and histomorphometric markers of bone turnover.

Methods

The study was approved by the Ethics Committee of the Hospital District of South Western Finland and was conducted in accordance with the Declaration of Helsinki as revised 1966. All subjects gave written informed consent.

Study subjects

The study subjects were recruited from the Turku University Hospital Kidney Center. The inclusion criteria were as follows: end-stage kidney disease (ESKD) and ongoing maintenance dialysis, and long-term elevated PTH and hyperphosphatemia indicating mineral and bone disorder. The exclusion criteria were pregnancy and administration of bisphosphonate medication in the past 6 months. The medication for secondary

hyperparathyroidism remained unchanged during the study period. All patients underwent an [^{18}F]NaF PET-CT scan including a CT scan of the heart. Bone biopsy was performed as a part of the study protocol 4–6 weeks after the PET scan.

Radiopharmaceutical spesifics

The radionuclide [^{18}F]fluoride ([^{18}F]F$^-$) was produced using a cyclotron by 11 MeV proton irradiation of ^{18}O-enriched water. The irradiated water containing [^{18}F]F$^-$ was applied to a preconditioned solid phase extraction cartridge using an automated device in a lead shielded hot cell. The cartridge was washed with sterile water to remove contaminants and traces of irradiated water. Finally, [^{18}F]F$^-$ was eluted from the cartridge with saline. This solution is formulated for injection using sterile filtration through sterile filters. The quality control tests for the tracer conform to the European Pharmacopeia.

[^{18}F]-Sodium fluoride positron emission tomography

We used a Discovery VCT scanner (GE Healthcare) to obtain the PET scans. The scanner had an axial field of view of 15 cm. A 60-minute dynamic scan of the lumbar spine (LS) and a 10-minute static scan of the pelvis were performed. The tracer (200 MBq [^{18}F]NaF) was injected the moment the PET scan started. Images were reconstructed by filtered back-projection, resulting in 42 × 3.27 mm slices for each frame. ROIs in the LS and the pelvis were defined by drawing an ROI within each vertebral body and on the anterior iliac crest (AIC). The same ROIs were used for calculating SUV. As arterial input function, we used an image-derived input function by placing an ROI over the abdominal aorta [23, 24]. Image derived AIFs can present technical challenges and extra caution was attended when drawing the aorta ROI, see Additional file 1. The method is described in detail in a previous publication [4].

Data analysis

The calculations were performed using the medical image analysis software CARIMAS, which was developed in Turku PET Centre to facilitate the interpretation of experimental PET scans (https://turkupetcentre.fi/carimas/carimasce/) [25].

Patlak analysis

The Patlak plot is a graphical analysis technique widely used when analyzing dynamic PET scans using the tracer [^{18}F]F$^-$ [1, 16, 19]. This technique requires that free [^{18}F]F$^-$ in bone can form a dynamic balance with [^{18}F]F$^-$ in blood and that [^{18}F]F$^-$ bound to the bone mineral compartment stays there during the time of measurements. (Patlak plot only becomes linear when both of these assumptions are valid). To estimate the fluoride bone influx rate, k_i following equation is used:

$$\frac{C_t\,(t)}{C_b\,(t)} = K_i \left[\frac{\int_0^t C_b\,(t)\,dt}{C_b\,(t)}\right] + V$$

Using ROI approach, tissue activity concentration is $C_t(t)$ at time t and the blood concentration of the tracer is $C_b(t)$. V is the effective distribution volume (mL/mL) of the tracer. Assuming fluoride is irreversibly bound to bone, the net influx rate of fluoride to bone is K_i (mL/min/mL).

In the static scan of the hip, the FUR is an approximation of Patlak K_i [26]. The ROI was drawn in the same region from where the bone biopsy was obtained. To calculate FUR, bone activity concentration by the area under the curve (AUC) of blood activity is divided from [^{18}F]F$^-$ administration time to the time of static scan.

SUV

Standardized uptake values (SUVs) can be measured by normalizing the mean concentration of the tracer [^{18}F]F$^-$ in the bone ROI for body weight and injected activity [19, 27]. SUV_{mean} was calculated using the following formula:

$$SUV = \frac{C_t\,(t)}{ID/m}$$

Ct(t) is the mean tissue activity, *ID* the injected dose and m the patient´s body weight. SUV was calculated within three frames (48–60 min from the start of the dynamic scan). [^{18}F]F$^-$ concentration in bone is relatively stable during the last ten minutes of the 60-minute scan; therefore, the SUV was calculated in the three last frames of the dynamic scan, Additional file 3.

We adjusted the SUV_{mean} of the lumbar spine (L1-L4) to the mean uptake of fluoride in blood 48–60 min from initiation of the dynamic PET scan → SUV ratio (SUVR).

$$SUVR = \frac{\text{SUV mean}}{\text{SUV}_{\text{aorta}}}$$

Blood pharmacokinetics

The elimination rate constant (k_{EL}) was estimated by plotting the natural logarithm of tracer concentration in blood against time from injection and fitting the line to the linear end phase of the plot. This method was also used to estimate the AUC after the last measurement of the aorta concentration at 60 min. The total blood $AUC_{0-\infty}$ was used to calculate total blood clearance (CL_T) as

$$CL_T = \frac{ID}{AUC_{0-\infty}}$$

Coronary tomography

All the participants underwent a CT scan of the heart and coronary arteries (using GE Discovery VCT 48-slice CT/positron emission tomography device (GE Healthcare) prior to [^{18}F]NaF PET. The coronary artery calcification score (CAC) was calculated using the Agatston method for each coronary artery [28] expressed in modified Agatston units (AU).

Bone histomorphometry

Iliac crest biopsies were performed vertically under local anesthesia after double labeling with fluorochrome (tetracycline 500 mg x 3 po for two days, which was repeated after a drug free interval of ten days). The biopsy was obtained 7–10 days after the second label using a Snare-coil Mermaid Medical RBN-86 8G (3.3 mm) x 15 cm needle. Bone biopsies were fixed in 70% ethanol for at least 48 h before embedding in polymethylmethacrylate. A semiautomatic image analyzer (Bioquant Osteo II, Bioquant Image Analysis Corporation, Nashville, TN, USA) was used to analyze all parameters. If there was only a single tetracycline label, a value for MAR of 0.3 µm/day was used [29]. The method is described in detail in a previous publication [4]. Normal turnover values were set using the results of Recker et co (mean ± 1SD) [30, 31]: men: BFR/BS 3.6–18.8 µm/y and Ac.f 0.12–0.6, postmenopausal women: BFR/BS 6–22 µm/y and Ac.f 0.11–0.49/y, premenopausal women: BFR/BS 3–13 µm/y and Ac.f 0.04–0.26/y.

Table 1 Demographics, disease characteristics and medication of the study group

No. of patients	28
Female sex (%)	13 (46)
Age, **y** (median, range)	64 (37–83)
BMI (mean, SD)	24 (3.6)
History of diabetes (%)	12 (39)
Dialysis vintage, month (median, range)	10 (3–94)
Dialysis modality (PD/HD) (%)	50/50
Laboratory parameters	
fS-calcium-ion 1.16 mmol/l – 1.30 mmol/l (mean, SD))	1.17 (0.08)
fP-phosphorus 0.71–1.23 mmol/l (median, IQR)	1.69 (0.49)
fP-iPTH 15–65 ng/l (median, IQR)	285 (185–520)
P- D-25 > 50 nmol/l (median, IQR)	70 (44–91)
S- D- 1,25 37–216 pmol/l (median, IQR)	30 (24–55)
CAC score (median, IQR)	366 (111–656)
Bone histomorphometry	
High turnover/hyperparathyreoid bone disease	11 (42)
Normal turnover/mild hyperparathyroid bone disease	9 (35)
Low turnover/adynamic bone disease	6 (23)
Medication	
Alfacalcidol, Paricalcitol (%)	18 (64)
Calcium carbonate (%)	24 (86)
Calcimimetic (%)	4 (14)
Cholecalciferol (%)	25 (89)
Sevelamer/lantane carbonate (%)	17 (60)

Laboratory assessment

Serum ionized calcium, phosphate, 25-hydroxyvitamin D, 1,25-dihydroxyvitamin D and intact parathyroid hormone were performed in all patients. Laboratory tests were performed and analyzed by the Turku University Hospital central laboratory (TYKSLAB).

Statistical analysis

Statistical analyses for background variables were performed using SAS 9.4 for Windows and JMP Pro 14. Normality tests for bone histomorphometric and [^{18}F]NaF PET were performed visually together with the Shapiro–Wilk test. Nonparametric statistical tests were used if the parameters failed the normality test. The characteristics of the study population are expressed as median and interquartile range (IQR) or mean and standard deviation (SD). Correlations between bone turnover parameters and fluoride activity in the PET scan were assessed using the Spearman rank correlation test. Plasma clearance and bone uptake were compared according to turnover using the Wilcoxon test. P values less than 0.05 (two-tailed) were considered statistically significant.

Results

General

The study group comprised 28 patients on maintenance dialysis. The mean age was 64 years, and 13 (46%) were female. 50% were on peritoneal dialysis, and 50% were on hemodialysis. Patient demographics, kidney disease characteristics and medication are presented in Table 1.

A sufficient bone biopsy was obtained in 26 patients. According to histomorphometric parameters, 23% had low turnover bone disease, 35% normal turnover and 42% high turnover (Table 1). The patient demographics of each patient separately are shown in the supplements, Additional file 2.

PET studies

Blood clearance to bone, $K_{i,}$ standardized bone uptake, SUV, were measured in the LS (L1–L4), and a mean value was calculated. In addition, SUV and FUR were measured at the AIC. The $K_{i\ mean}$ and SUV_{mean} were compared with histomorphometric parameters using the Spearman rank correlation test (Table 2). There was a statistically significant correlation between the $K_{i\ mean}$ in the LS and FUR at the AIC and histomorphometric parameters measuring bone turnover (bone formation rate,

Table 2 Correlation between histomorphometric markers and bone uptake and blood clearance to bone values

Histomorphometry	$K_{i\ mean}$ L1-L4	SUV_{mean} L1-L4	FUR_{mean} hip	SUV_{mean} hip	SUVR
Bone formation rate	$r_s = 0.64, p < 0.001$	$p = 0.23$	$r_s = 0.67, p < 0.001$	0.21	$r_s = 0.57, p = 0.003$
Activation Frequency	$r_s = 0.64, p < 0.001$	$p = 0.29$	$r_s = 0.68, p < 0.001$	0.13	$r_s = 0.60, p = 0.002$
Osteoclast activity	$r_s = 0.54, p = 0.004$	$p = 0.59$	$r_s = 0.66, p < 0.001$	0.11	$r_s = 0.66, p = 0.008$
Osteoblast activity	$r_s = 0.65, p < 0.001$	$p = 0.11$	$r_s = 0.62, p < 0.001$	0.57	$r_s = 0.339, p = 0.05$
Erosion surface per bone surface	$r_s = 0.62, p < 0.001$	$r_s = 0.45, p = 0.02$	$r_s = 0.64, p < 0.001$	$r_s = 0.46, p = 0.02$	$r_s = 0.61, p = 0.001$
Mineralized surface per bone surface	$r_s = 0.52, p = 0.005$	$p = 0.32$	$r_s = 0.53, p = 0.005$	0.23	$r_s = 0.61, p = 0.005$
Bone uptake SUV_{mean} L1-L4	$r_s = 0.55, p = 0.006$	-	$r_s = 0.52, P = 0.005$	$r_s = 0.78, P < 0.001$	$r_s = 0.56, p < 0.002$

Table 3 Blood clearance to bone and standardized bone uptake values according to turnover in dialysis patients

	Low turnover *n* = 6	Normal turnover *n* = 9	High turnover *n* = 11	*p* - value
K_i (mL/min/mL)				
L1	0.034 (0.026–0.038)	0.049 (0.036–0.045)	0.056 (0.053–0.065)	0.001
L2	0.032 (0.027–0.037)	0.037 (0.035–0.048)	0.057 (0.053–0.063)	0.003
L3	0.030 (0.023–0.030)	0.038 (0.036–0.046)	0.058 (0.051–0.078)	< 0.001
L4	0.032 (0.026–0.037)	0.041 (0.036–0.046)	0.057 (0.048–0.075)	0.005
SUV (g/ml)				
L1	5.4 (4.9–7.7)	6.4 (5.0–7.6)	7.8 (6.6–8.7)	0.3
L2	5.0 (4.4–7.8)	5.7 (5.1–7.5)	7.4 (6.1–8.2)	0.2
L3	4.8 (4.1–7.6)	5.9 (4.9–7.2)	7.1 (5.5–8.1)	0.2
L4	5.1 (4.6–7.6)	6.2 (5.0–7.1)	7.7 (5.2–8.1)	0.2
SUVR				
L1 - L4	3.0 (2.3–3.8)	4.2 (2.8–4,4)	5.0 (3.9–6.1)	0.02
FUR_{mean}(mL/min/mL)				
Hip	0.033 (0.029–0.038)	0.041 (0.035–0.048)	0.060 (0.050–0.071)	0.002
SUV_{mean} (g/ml)				
Hip	5.9 (4.6–7.4)	5.9 (5.5–7.0)	7.7 (6.8–9.8)	0.04*

Variables are reported as median and interquartile range. Reported p values are based on comparison between high and low turnover/normal turnover. * The p value of SUV_{mean} hip is significant, but when doing pairwise comparison using Tukey´s method, there was no significant difference between the groups. SUVR reflects mean bone uptake in the lumbar spine corrected by mean blood uptake of fluoride 48–60 min fron initiation of the dynamic PET scan. Reported p values are based on comparisons between high and low bone turnover

activation frequency, osteoblast and osteoclast activity, erosion surface and mineralized surface). SUV_{mean} (L1-L4) correlated weakly with erosion surface ($p = 0.02$, $r_s = 0.46$), but there was no statistically significant correlation with other histomorphmetric parameters (Table 2). SUV_{mean} was adjusted with CAC, but this did not impact the result. However, the SUVR of the LS significantly correlated with histomorphometric parameters (Table 2) and blood clearance to bone, K_i, $r_s = 0.92$ and $p < 0.001$,

Blood clearance to bone and standardized bone uptake in vertebras L1–L4 according to turnover are shown in Table 3. K_i and SUVR were significantly higher in high-turnover bone disease than in low-turnover bone disease, but there was no statistically significant difference between SUVs in different turnover groups. The mean k_i in patients with low turnover was 0.032 (0.029–0.037), SUV_{mean} was 5.1 (4.5–7.9) and SUVR was 3.0 (2.3–3.8). In patients with normal turnover, the $_{mean}$ K_i was 0.038 (0.037–0.047), SUV_{mean} was 6.2 (5.1–7.5) and SUVR was 4.2 (2.8–4.4), and in patients with high turnover, the $_{mean}$ K_i was 0.056 (0.051–0.067), SUV_{mean} was 7.4 (6.0–8.5) and SUVR was 5.0 (3.9–6.1).

We calculated total blood clearance of fluoride CL_T and elimination rate of fluoride, k_{EL}. No significant difference in CL_T and k_{EL} was seen in patients with high or low turnover bone disease or in patients with normal turnover. Figure 1 shows the ratio of bone and blood uptake of fluoride in the LS. The ratio continues to increase 1 h from the initiation of the dynamic PET scan.

In Additional file 3, the TACs in dynamic [^{18}F]NaF PET scan for both bone and blood in a patient with high-turnover bone disease, a patient with low-turnover bone disease and a patient with normal turnover based on bone biopsies are shown. The bone and blood curves diverge at different time points depending on the underlying bone disease. In high-turnover bone disease, bone uptake increases rapidly at the beginning of the scan. In low-turnover bone disease, the increase is slower. In the last 10 min of the scan, the TACs are straight, and changes in tracer uptake are small.

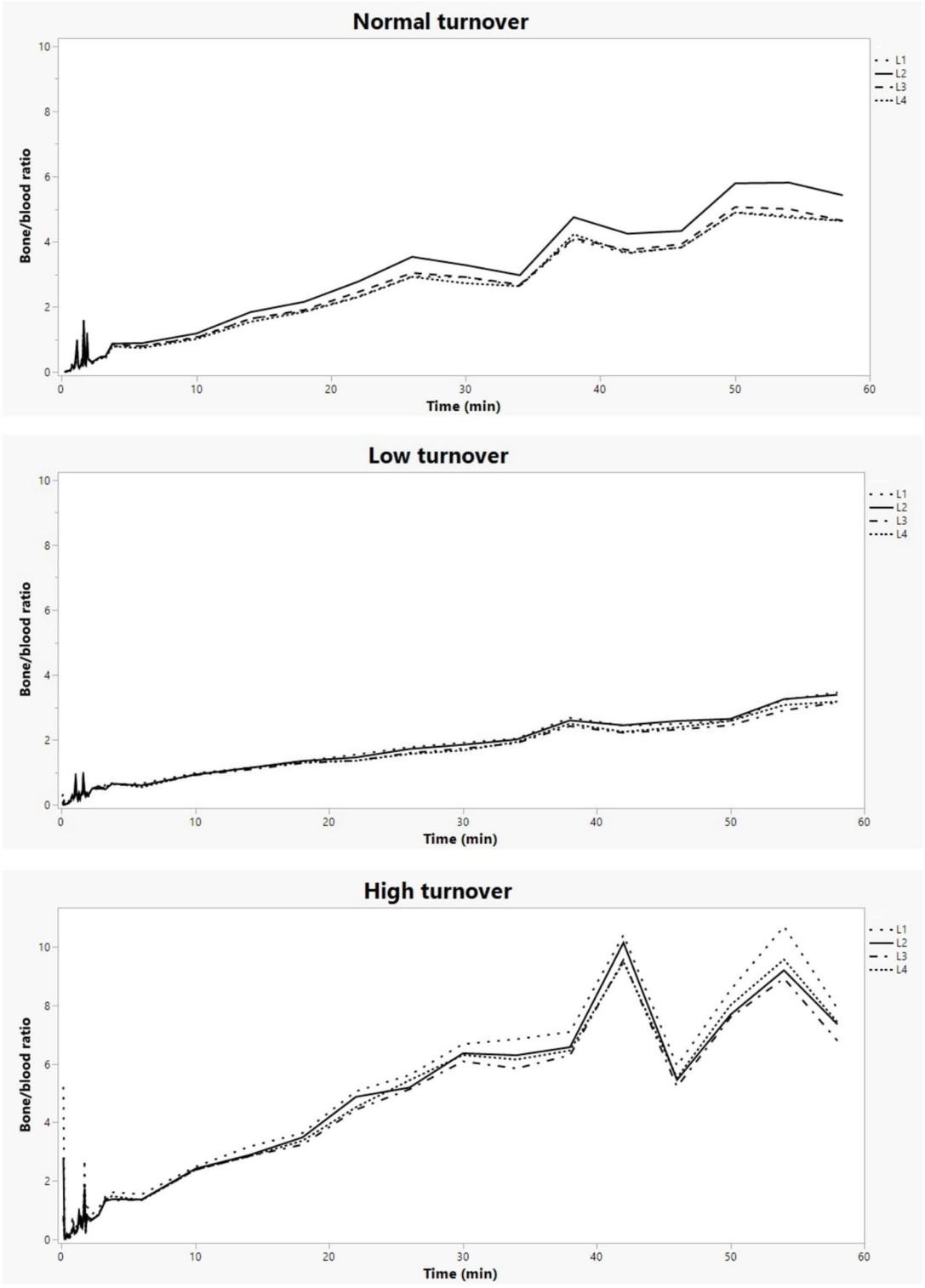

Fig. 1 The ratio between bone and blood uptake of $^{18}F^-$ in the different categories of renal osteodystrophy

Discussion

In the present study, blood clearance to bone using dynamic PET scans was compared to standardized bone uptake values measured 48–60 min after tracer injection. As a reference test of bone metabolism, we used histomorphometric parameters from the bone biopsy. We have previously shown a clear correlation between histomorphometric parameters measuring bone metabolism

and dynamic [^{18}F]NaF PET [4, 7]. The ability of [^{18}F]NaF PET to distinguish between low- and high-turnover bone disease in dialysis patients is good [7]. When measuring SUVs in the same study population, there was no correlation with histomorphometric parameters and SUV was not able to distinguish between the subgroups of renal osteodystrophy. Adjustment for the coronary calcification score did not affect the results. However, when adjusting tracer activity in bone to tracer activity measured from the aorta 48–60 min after injection, SUVR correlated strongly with K_i.

An non-invasive imaging method evaluating bone metabolism would be a valuable tool of the highest value and desperately warranted in clinical practice. Static scans are short and easier both for the patients and the imaging units. SUVs cannot be used when evaluating extensive bone disease in CKD patients. In PET imaging using ^{18}F-FDG, approximately 10% of the injected dose is excreted into urine 70 min after the injection, but the excretion is highly variable [32]. There are no studies evaluating the impact of kidney function, residual function and urine excretion on tracer uptake into bone in ESKD patients. A method where blood clearance to bone is estimated from static scans following one injection of tracer would be an alternative approach to circumvent the problem of dynamic scans. We divided mean bone uptake in L1–L4 by the mean blood uptake 48–60 min after injection, resulting in a strong correlation with K_i. This indicates that static scans obtained 60 min from the tracer injection together with blood samples 48 and 60 min from injection could generate usable images for bone metabolism assessment at several sites of the skeleton. Image-derived AIF cannot be reliably obtained from static scans, which is why venous blood samples might be a better option.

Siddique et al. proposed a simplified method where bone plasma clearance of [^{18}F]F^- could be estimated from a static scan after a single injection of tracer [33]. In their study, blood samples were obtained at 30, 40, 50 and 60 min after tracer injection and static images 30–60 min after tracer injection. K_i was evaluated using the Patlak analysis and the static method. Measurement of k_i from the static scans 30–60 min after injection correlated highly with the Patlak results ($r > 0.99$). Siddique et al. also proposed a method using a modified analysis that corrects ^{18}F efflux from bone up to 2 h from injection, enabling multiple static scans [34].

[^{18}F]NaF PET is increasingly used in research settings to assess arterial deposition and has been used in the research of atherosclerotic disease and diffuse medial calcification [35–37]. An inverse correlation between the activity of arterial mineral deposition and regional bone metabolism measuring standardized bone uptake has been shown in one study [22]. To what extent the tracer uptake into arterial depositions affects standardized bone uptake is not known. This study population was rather old with multiple comorbidities and extensive atherosclerotic disease. However, based on our results, the grade of CAC did not impact the bone uptake values of fluoride measured by [^{18}F]NaF PET.

Standardized bone uptake measurements are used in oncology to express tracer uptake in tumors [38]. Usually, the maximum SUV within heterogeneous tumors is reported. In studies of extensive metabolic disease, such as osteoporosis, tracer uptake in bone is more uniform, and therefore, mean SUV values are used. The limitation of using standardized bone uptake is, that there is only a certain amount of tracer that all competing tissues share. Therefore, regional bone uptake not only reflects local demand of the tracer in the measured site, but also the competing areas of the skeleton influence the uptake [39]. For example, in the case of a systemic bone disease such as Paget's disease or treatment with a potent anabolic agent [20, 40], the arterial plasma concentration could be reduced by the increased tracer competition and the local bone uptake, thus reduced ("sink effect"). In renal osteodystrophy, similar challenges are possible. In high-turnover bone disease, metabolic activity and bone turnover are increased, and osteoblasts and osteoclasts are highly active, which could lead to reduced local tracer uptake of tracers because of increased competition. In low-turnover bone disease, the metabolic activity in bone is decreased, osteoblastic activity is very low, and SUVs might overestimate metabolic activity in the bone because the proportional amount of available tracer available is larger.

In our study population, 23% had low-turnover bone disease and 42% had high-turnover bone disease based on histomorphometric markers obtained by bone biopsy. We calculated the fluoride elimination rate from blood, $k_{EL,}$ and the total blood clearance, CL_T, to assess the impact of the type of disturbance in bone metabolism (high turnover versus low turnover) on fluoride elimination and blood clearance. Surprisingly, there were no significant differences between the different turnover groups. Thus, the so-called sink effect could not be observed in this study population, or was rendered indiscernible by other conditions. This study population consisted of maintenance dialysis patients, and the residual function of the kidneys and the amount of urine per day were not documented. The results of this study suggest that possible residual kidney function and urine secretion cause a wide dispersion in SUV values, which nullifies the differences in different bone turnover groups, not the differences in fluoride elimination from blood or blood clearance. This indicates that in patients with CKD or in patients on maintenance dialysis, the reliability of using standardized bone uptake in PET imaging using the

tracer $^{18}F^-$ requires further research and validation of the method.

In the research of metabolic diseases, radionuclide imaging of the skeleton using the tracer [^{18}F]F^- is a valuable tool. It enables in a unique way studies of regional bone metabolism that reflect bone remodeling and bone blood flow [18, 41]. Quantitative [^{18}F]NaF PET studies are usually performed using the dynamic scan method where AIF is needed to measure blood clearance of tracer to bone. In dynamic quantitative scans, the rate of tracer uptake into an organ is normalized by its concentration in arterial blood. The need for AIF, however, creates challenges in clinical use. The liver is a plethoric organ and could work, being in the imaging frames of dynamic scans, but this needs further research.

A number of limitations and potential sources of inaccuracies need to be considered. This study population was rather small and heterogeneous. The patients had multiple comorbidities, the age range was wide and residual kidney function or urine output were unknown Additionally, the fact that we used an image-derived AIF instead of an arterial blood line is a limitation, even though there were reasonable arguments to do so.

Conclusions

In conclusion, our study suggests that tracer activity in the blood obtained 48–60 min after injection of the tracer can be used to correct SUVs from static [^{18}F]NaF PET scans. This method does not reach the diagnostic accuracy of a 60-minute dynamic [^{18}F]NaF PET scan but could be a feasible method in clinical practice. In this study, image-derived AIFs was used, but these results indicate that also venous blood measurements obtained 48–60 min after tracer injection could be used. This, however, requires further research and validation of the method using both image- and venous blood-derived AIFs.

Abbreviations

[^{18}F]NaF PET	[^{18}F]- Sodium Fluoride positron emission tomography
SUV	Standardized uptake values
SUVR	Standardized uptake values ratio
LS	Lumbar spine
AIC	Anterior iliac crest
K_i	Blood clearance of tracer to bone
TAC	Blood time activity curve
AIF	Arterial input function
ESKD	End-stage kidney disease
ROI	Region of interest
ID	Injected dose
M	Body weight of the patient
k_{EL}	Elimination rate constant
AUC	Area under the curve
CAC	Coronary artery calcification
AU	Agatston unit
MAR	Mineral apposition rate
IQR	Interquartile range
SD	Standard deviation

Supplementary Information

The online version contains supplementary material available at https://doi.org/10.1186/s12882-025-04063-w.

Supplementary Material 1

Acknowledgements

Not applicable.

Author contributions

Louise Aaltonen: conceptualization, data curation, formal analysis, investigation, visualization and writing-original draft. Niina Koivuviita: conceptualization, supervision, writing-review and editing. Vesa Oikonen: methodology, writing-review and editing. Marko Seppänen: methodology, writing-review and editing. Anna Kirjavainen: methodology. Heikki Kröger: methodology writing-review and editing. Eliisa Löyttöniemi: Formal analysis, writing-review and editing. Kaj Metsärinne: Conceptualization, Funding acquisition, Project administration, Supervision, Writing-review & editing. All the authors have read and approved the final manuscript.

Funding

This work was supported by the Finska Läkaresällskapet, Munuaissäätiö and the Perklén Foundation, Helsinki, Finland.

Data availability

The data that support the findings of this study are available from the corresponding author upon reasonable request.

Declarations

Ethics approval and consent to participate

All procedures performed in this study were in accordance with ethical standards of the institutional review board. The study was approved by the Ethics Committee of the Hospital District of South Western Finland and was conducted in accordance with the 1964 Declaration of Helsinki and its later amendments.

Consent to participate

Informed consent was obtained from all individual participants included in the study.

Consent for publication

Not applicable.

Competing interests

The authors declare no competing interests.

Author details

[1]Kidney Center, Department of Medicine, Turku University Hospital, PL 52, Kiinamyllynkatu 4-8, Turku 20521, Finland
[2]Turku PET Centre, University of Turku, Kiinamyllynkatu 4-8, Turku 20521, Finland
[3]Department of Clinical Physiology, Nuclear Medicine, Turku University Hospital, PL 52, Kiinamyllynkatu 4-8, Turku 20521, Finland
[4]Radiopharmaceutical Chemistry Laboratory, Turku PET Centre, University of Turku, Turku, Finland
[5]Kuopio University Hospital and University of Eastern Finland, Kuopio, Finland
[6]Department of Biostatistics, University of Turku, Kiinamyllynkatu 10, Turku 20014, Finland

Received: 15 February 2024 / Accepted: 8 March 2025
Published online: 02 April 2025

References

1. Hawkins RA, Choi Y, Huang SC, et al. Evaluation of the skeletal kinetics of fluorine-18-fluoride ion with PET. J Nucl Med. 1992;33(5):633–42.

2. Moore AE, Blake GM, Taylor KA, et al. Changes observed in radionuclide bone scans during and after teriparatide treatment for osteoporosis. Eur J Nucl Med Mol Imaging. 2012;39(2):326–36. https://doi.org/10.1007/s00259-011-1974-y.
3. Czernin J, Satyamurthy N, Schiepers C. Molecular mechanisms of bone 18F-NaF deposition. J Nucl Med. 2010;51(12):1826–9. https://doi.org/10.2967/jnumed.110.077933.
4. Aaltonen L, Koivuviita N, Seppanen M, et al. Correlation between (18) F-sodium fluoride positron emission tomography and bone histomorphometry in dialysis patients. Bone. 2020;134:115267. https://www.sciencedirect.com/science/article/pii/S8756328220300478.
5. Piert M, Zittel TT, Becker GA, et al. Assessment of porcine bone metabolism by dynamic. J Nucl Med. 2001;42(7):1091–100.
6. Messa C, Goodman WG, Hoh CK, et al. Bone metabolic activity measured with positron emission tomography and [18F]fluoride ion in renal osteodystrophy: correlation with bone histomorphometry. J Clin Endocrinol Metab. 1993;77(4):949–55. https://doi.org/10.1210/jcem.77.4.8408470.
7. Aaltonen L, Koivuviita N, Seppanen M, et al. Bone histomorphometry and (18)F-sodium fluoride positron emission tomography imaging: comparison between only bone turnover-based and unified TMV-based classification of renal osteodystrophy. Calcif Tissue Int. 2021;109(6):605–14. https://doi.org/10.1007/s00223-021-00874-9.
8. Sprague SM, Bellorin-Font E, Jorgetti V, et al. Diagnostic accuracy of bone turnover markers and bone histology in patients with CKD treated by dialysis. Am J Kidney Dis. 2016;67(4):559–66. https://doi.org/10.1053/j.ajkd.2015.06.023.
9. Guerin AP, London GM, Marchais SJ, Metivier F. Arterial stiffening and vascular calcifications in end-stage renal disease. Nephrol Dial Transpl. 2000;15(7):1014–21. https://doi.org/10.1093/ndt/15.7.1014.
10. Kidney Disease: Improving Global Outcomes (KDIGO) CKD-MBD Work Group. KDIGO clinical practice guideline for the diagnosis, evaluation, prevention, and treatment of chronic kidney disease-mineral and bone disorder (CKD-MBD). Kidney Int Suppl. 2009;113S1–130. https://doi.org/10.1038/ki.2009.188.
11. Barreto DV, Barreto Fde C, Carvalho AB, et al. Association of changes in bone remodeling and coronary calcification in hemodialysis patients: a prospective study. Am J Kidney Dis. 2008;52(6):1139–50. https://doi.org/10.1053/j.ajkd.2008.06.024.
12. Miller PD. The role of bone biopsy in patients with chronic renal failure. Clin J Am Soc Nephrol. 2008;3(Suppl 3):140. https://doi.org/10.2215/CJN.02430508.
13. Ott SM. Histomorphometric measurements of bone turnover, mineralization, and volume. Clin J Am Soc Nephrol. 2008;3:151. https://doi.org/10.2215/CJN.04301206.
14. Salam S, Gallagher O, Gossiel F, Paggiosi M, Khwaja A, Eastell R. Diagnostic accuracy of biomarkers and imaging for bone turnover in renal osteodystrophy. J Am Soc Nephrol. 2018;29(5):1557–65. https://doi.org/10.1681/ASN.2017050584.
15. Park-Holohan SJ, Blake GM, Fogelman I. Quantitative studies of bone using (18)F-fluoride and (99 m)tc-methylene diphosphonate: evaluation of renal and whole-blood kinetics. Nucl Med Commun. 2001;22(9):1037–44. https://doi.org/10.1097/00006231-200109000-00014.
16. Patlak CS, Blasberg RG, Fenstermacher JD. Graphical evaluation of blood-to-brain transfer constants from multiple-time uptake data. J Cereb Blood Flow Metab. 1983;3(1):1–7. https://doi.org/10.1038/jcbfm.1983.1.
17. Ishizu K, Nishizawa S, Yonekura Y, et al. Effects of hyperglycemia on FDG uptake in human brain and glioma. J Nucl Med. 1994;35(7):1104–9.
18. Blake GM, Siddique M, Frost ML, Moore AE, Fogelman I. Imaging of site specific bone turnover in osteoporosis using positron emission tomography. Curr Osteoporos Rep. 2014;12(4):475–85. https://doi.org/10.1007/s11914-014-0231-2.
19. Brenner W, Vernon C, Muzi M, et al. Comparison of different quantitative approaches to 18F-fluoride PET scans. J Nucl Med. 2004;45(9):1493–500. https://jnm.snmjournals.org/content/45/9/1493.short.
20. Blake GM, Siddique M, Frost ML, Moore AE, Fogelman I. Radionuclide studies of bone metabolism: do bone uptake and bone plasma clearance provide equivalent measurements of bone turnover? Bone. 2011;49(3):537–42. https://doi.org/10.1016/j.bone.2011.05.031.
21. Irkle A, Vesey AT, Lewis DY, et al. Identifying active vascular microcalcification by (18)F-sodium fluoride positron emission tomography. Nat Commun. 2015;6:7495. https://doi.org/10.1038/ncomms8495.
22. Derlin T, Janssen T, Salamon J, et al. Age-related differences in the activity of arterial mineral deposition and regional bone metabolism: an 18F-sodium fluoride positron emission tomography study. Osteoporos Int. 2015;26(1):199–207. https://doi.org/10.1007/s00198-014-2839-6.
23. Cook GJ, Lodge MA, Marsden PK, Dynes A, Fogelman I. Noninvasive assessment of skeletal kinetics using fluorine-18 fluoride positron emission tomography: evaluation of image and population-derived arterial input functions. Eur J Nucl Med. 1999;26(11):1424–9. https://link.springer.com/article/10.1007/s002590050474.
24. Puri T, Blake GM, Frost ML, et al. Validation of image-derived arterial input functions at the femoral artery using 18F-fluoride positron emission tomography. Nucl Med Commun. 2011;32(9):808–17. https://doi.org/10.1097/MNM.0b013e328349716f.
25. Carimas: an extensive medical imaging data processing tool for research. https://doi.org/10.1007/s10278-023-00812-1
26. Thie JA. Clarification of a fractional uptake concept. J Nucl Med. 1995;36(4):711–2.
27. Uchida K, Nakajima H, Miyazaki T, et al. Effects of alendronate on bone metabolism in glucocorticoid-induced osteoporosis measured by 18F-fluoride PET: a prospective study. J Nucl Med. 2009;50(11):1808–14. https://doi.org/10.2967/jnumed.109.062570.
28. Agatston AS, Janowitz WR, Hildner FJ, Zusmer NR, Viamonte M, Detrano R. Quantification of coronary artery calcium using ultrafast computed tomography. J Am Coll Cardiol. 1990;15(4):827–32. https://doi.org/10.1016/0735-1097(90)90282-T.
29. Dempster DW, Compston JE, Drezner MK, et al. Standardized nomenclature, symbols, and units for bone histomorphometry: a 2012 update of the report of the ASBMR histomorphometry nomenclature committee. J Bone Min Res. 2013;28(1):2–17. https://doi.org/10.1002/jbmr.1805.
30. Recker RR, Akhter MP, Lappe JM, Watson P. Bone histomorphometry in transiliac biopsies from 48 normal, healthy men. Bone. 2018;111:109–15. https://www.sciencedirect.com/science/article/abs/pii/S8756328218301388.
31. Recker RR, Lappe JM, Davies M, Kimmel D. Perimenopausal bone histomorphometry before and after menopause. Bone. 2018;108:55–61. https://www.sciencedirect.com/science/article/abs/pii/S8756328217304726.
32. Bach-Gansmo T, Dybvik J, Adamsen T, Naum A. Variation in urinary excretion of FDG, yet another uncertainty in quantitative PET. Acta Radiol Short Rep. 2012;1(8):https://doi.org/10.1258/arsr.2012.120038. eCollection 2012.
33. Siddique M, Blake GM, Frost ML, et al. Estimation of regional bone metabolism from whole-body 18F-fluoride PET static images. Eur J Nucl Med Mol Imaging. 2012;39(2):337–43. https://doi.org/10.1007/s00259-011-1966-y.
34. Siddique M, Frost ML, Moore AE, Fogelman I, Blake GM. Correcting (18) F-fluoride PET static scan measurements of skeletal plasma clearance for tracer efflux from bone. Nucl Med Commun. 2014;35(3):303–10. https://doi.org/10.1097/MNM.0000000000000047.
35. Joshi NV, Vesey AT, Williams MC, et al. 18F-fluoride positron emission tomography for identification of ruptured and high-risk coronary atherosclerotic plaques: a prospective clinical trial. Lancet. 2014;383(9918):705–13. https://doi.org/10.1016/S0140-6736(13)61754-7.
36. Derlin T, Richter U, Bannas P, et al. Feasibility of 18F-sodium fluoride PET/CT for imaging of atherosclerotic plaque. J Nucl Med. 2010;51(6):862–5. https://doi.org/10.2967/jnumed.110.076471.
37. Janssen T, Bannas P, Herrmann J, et al. Association of linear (1)(8)F-sodium fluoride accumulation in femoral arteries as a measure of diffuse calcification with cardiovascular risk factors: a PET/CT study. J Nucl Cardiol. 2013;20(4):569–77. https://doi.org/10.1007/s12350-013-9680-8.
38. Keyes JW. SUV: standard uptake or silly useless value? J Nucl Med. 1995;36(10):1836–9.
39. Blake GM, Moore AE, Fogelman I. Quantitative studies of bone using (99 m) tc-methylene diphosphonate skeletal plasma clearance. Semin Nucl Med. 2009;39(6):369–79. https://doi.org/10.1053/j.semnuclmed.2009.05.001.
40. Gnanasegaran G, Moore AE, Blake GM, Vijayanathan S, Clarke SE, Fogelman I. Atypical paget's disease with quantitative assessment of tracer kinetics. Clin Nucl Med. 2007;32(10):765–9. https://doi.org/10.1097/RLU.0b013e318148b1dd.
41. Blake GM, Park-Holohan SJ, Cook GJ, Fogelman I. Quantitative studies of bone with the use of 18F-fluoride and 99mTc-methylene diphosphonate. Semin Nucl Med. 2001;31(1):28–49. https://www.sciencedirect.com/science/article/abs/pii/S0001299801800301.

Publisher's note